Available online at www.sciencedirect.com
SCIENCE DIRECT®
Mechanism and Machine Theory 40 (2005) 740–756
Mechanism and Machine Theory
www.elsevier.com/locate/mechmt

Kinematics analyses of Dodekapod

Prakash Bande [a], Martin Seibt [b], Eckart Uhlmann [b], S.K. Saha [c,*], P.V.M. Rao [c]

[a] *Altair Engineering, Bangalore, India*
[b] *Institute of Machine Tools, Technical University, Berlin, Germany*
[c] *Department of Mechanical Engineering, Indian Institute of Technology Delhi, Hauz Khas, New Delhi 110 016, India*

Received 14 September 2002; received in revised form 18 November 2004; accepted 23 November 2004
Available online 5 March 2005

Abstract

Dodekapod is a recent development in the area of parallel manipulators. It is a manipulator with 12 degree of freedom proposed as an alternative to six degree of freedom Hexapod, to overcome workspace limitations. This paper deals with the inverse and forward kinematics of Dodekapod. A hierarchical method to solve the kinematics is proposed assuming gripping as an end application. Using this approach, the problem of kinematics can be reduced to that of a general 6–6 Stewart platform for which solutions have been proposed in the past.
© 2005 Elsevier Ltd. All rights reserved.

Keywords: Dodekapod; Parallel manipulators; Stewart platform; Kinematics

1. Introduction

Parallel manipulators are being preferred for many applications, as they have advantages of higher stiffness, better accuracy, and dynamic capabilities over their serial counterparts. Dodekapod [1] is a recent addition to the family of parallel manipulators. Spur et al. [1] have proposed such a manipulator for gripping application, e.g., holding a washing machine while it is painted by, say, a robot. Unlike a Stewart platform type of manipulator, which has six degree of freedom,

* Corresponding author. Tel.: +91 11 2659 1135; fax: +91 11 2658 2053.
E-mail address: saha@mech.iitd.ernet.in (S.K. Saha).

0094-114X/$ - see front matter © 2005 Elsevier Ltd. All rights reserved.
doi:10.1016/j.mechmachtheory.2004.11.006

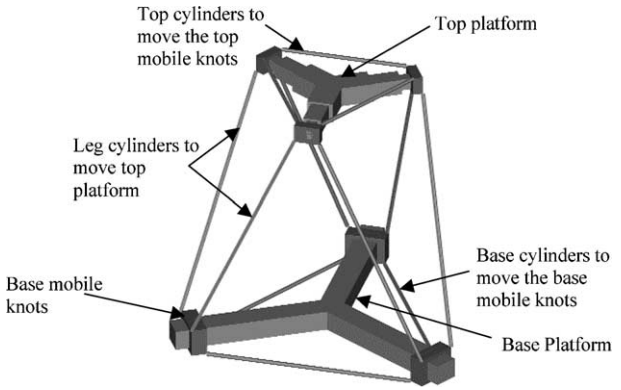

Fig. 1. Dodekapod.

Dodekapod has six additional degree of freedom. Fig. 1 shows a schematic sketch of Dodekapod. It has six legs like Hexapod which are connected to mobile knots at the top and base platforms. The mobile knots at the base platform can be moved along three sliders that are at an angle of 120° with one another. A similar arrangement at the top platform is achieved using telescopic guides. Dodekapod can be considered as a Hexapod with variable workspace. Additional degree of freedom, as available from the movement of the mobile knots of the top and bottom platforms, can be used for varying the workspace. Such a configuration has been explored for gripping applications, where the top platform of Dodekapod acts as a gripping platform. Detailed description of this mechanism can be found in [1,2]. Of the 12 degree of freedom of Dodekapod, six define the position and orientation of the top platform, three define the position of base mobile knots and the remaining three determine the position of top mobile knots. It may be noted that for gripping application, the position of top mobile knots are dictated by the object to be gripped, which accounts for three degrees of freedom. Hence the remaining three degree of freedom are redundant. For control and simulation of such systems, kinematic analyses of Dodekapod are proposed in this paper.

Since the development of Stewart platform [3,4] various authors have addressed the problems related to kinematics and dynamics of parallel manipulators [5–13]. It has been shown in [6–8] that the Stewart platform of general geometry has 40 distinct solutions. Solutions of the generalized Stewart–Gough platform are also obtained in [9].

1.1. Nomenclature

Referring to Fig. 2, which shows a kinematic structure of the Dodekapod, it may be noted that all joints other than the six leg joints can be grouped to lie in four distinct planes. Fig. 2 shows the grouping of these joints in planes a, b, c and d. Passive or unactuated joints in each plane are denoted by the alphabet identifying the plane with suffixes from 1 to 6 as there are six joints in each plane. For the purpose of kinematics analyses two right-hand coordinate frames are attached. The fixed reference frame B has its origin at the center of the base platform on plane b. Its Y_b-axis passes through the midpoint of line b_1b_6, Z_b-axis is normal to the plane b and the X_b-axis of the coordinate system is determined by the right hand rule. Similarly, the movable frame C has its origin on plane c, with its Y_c-axis passing through the midpoint of c_1c_2 and Z_c-axis being

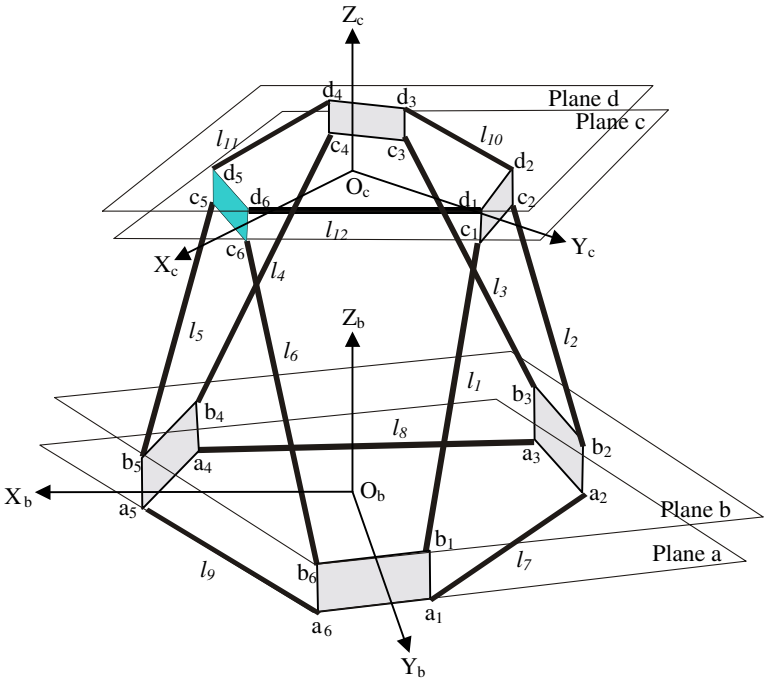

l_1…l_6: leg cylinders; l_7, l_8, l_9: base cylinders; l_{10}, l_{11}, l_{12}: top cylinders

Fig. 2. Nomenclature.

normal to plane *c*. Leg cylinders are numbered from 1 to 6, base cylinders from 7 to 9, and the top cylinders from 10 to 12, as shown in Fig. 2. All the cylinders can be actuated whenever required. For example, leg cylinders are used to manipulate the object whereas the base and top cylinders

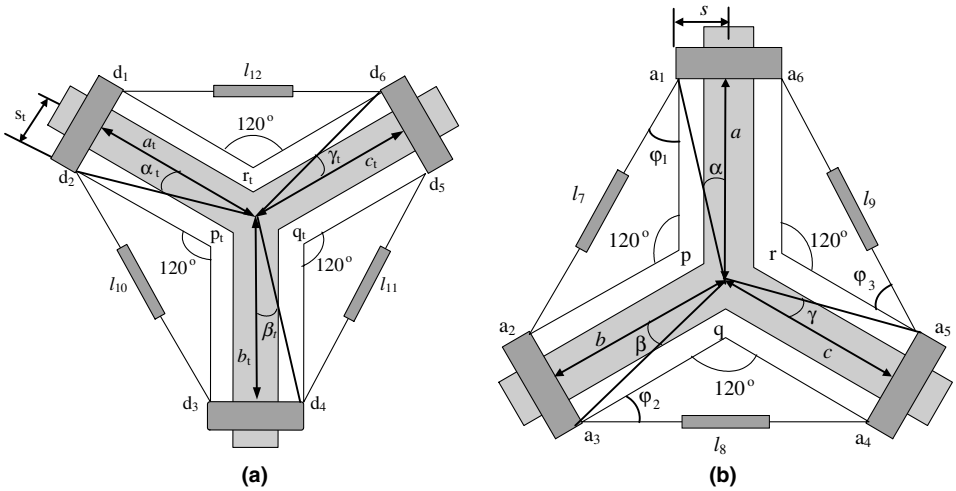

Fig. 3. (a) The top platform and (b) the base platform.

are used only when the adjustment has to be made for an object of different shape and size. Fig. 3 shows schematic diagram of the base and top platforms in detail.

The paper is organized as follows: Sections 2 and 3 provide the inverse and forward kinematics algorithms, respectively, whereas Section 4 gives the results of a numerical example. Finally, conclusions are given in Section 5.

2. Inverse kinematics

In the present kinematic analyses, it is assumed that the Dodekapod will be used as a positioning and gripping device. Keeping this in mind, the inverse kinematics problem of the Dodekapod can be stated as follows:

Given the position and orientation of the top platform and the positions of the top mobile knots which depend on the object to be gripped, determine the lengths of all the cylinders.

For any given gripping application, the top platform need to be positioned and orientated. The position and orientation of the top platform for this purpose can be described by defining a position vector $\mathbf{t}_c^b \equiv [x \quad y \quad z]^{\mathrm{T}}$, and rotation matrix $\mathbf{R}_c^b$ from frame C to frame B. The positions of the top mobile knots which are defined by their distances from the center of the top platform (shown as a_t, b_t and c_t in Fig. 3a), are dictated by the shape and size of the object to be gripped. So, input to our inverse kinematics problem are $\mathbf{t}_c^b$, $\mathbf{R}_c^b$, a_t, b_t and c_t. The other three degree of freedom of the Dodekapod in terms of the positions of the base mobile knots defined by their distances from the center of bottom platform, namely, a, b, and c in Fig. 3b are redundant resulting in infinite number of solutions to the inverse kinematics problem. In order to have a finite number of solutions, the method proposed here starts with assuming an initial configuration for the base mobile knots (a, b, and c). Problem of finding the leg lengths for this assumed configuration of the base mobile knots is equivalent to that of a general 6–6 Stewart platform inverse kinematics problem for which solutions have been proposed [6,8,9]. The feasibility of a solution in this case is first checked and if there is no feasible solution for the assumed configuration of the base mobile knots, the positions of the base mobile knots are changed. This process is repeated until a configuration of the base mobile knots gives a feasible solution. Thus, the inverse kinematics solution of the Dodekapod requires the following steps:

(i) Select an initial position of the base mobile knots, i.e., values a, b, and c.
(ii) Knowing a, b, and c, compute coordinates of each mobile knot.
(iii) Solve for leg lengths by solving the inverse kinematics problem of the 6–6 Stewart platform.
(iv) Verify the feasibility of the solutions, and change the position of the base mobile knots if necessary, till a feasible solution is found.

2.1. Step i

The initial position of the base mobile knots can be taken as the positions to which they adapt to when the three base cylinders are at their minimum or maximum lengths. That is, l_7, l_8 and l_9 are assumed to be known. From the geometry of Fig. 3b, note that

$$a_1p = a_6r, \quad a_3q = a_2p, \quad a_5r = a_4q \tag{1}$$

which can be expressed in terms of the values, a, b, c, and s of Fig. 3b, as shown in Eq. (A1) of Appendix A. Now, using the "sine rules" given in Eqs. (A2)–(A4), we get six linear transcendental equations in six variables, i.e., a_1p, a_3q, a_5r, and ϕ_1, ϕ_2, ϕ_3, as indicated in Fig. 3b. We shall now eliminate the variables, ϕ_1, ϕ_2, and ϕ_3, using the following relations:

$$\phi_1 = \mathrm{ArcCsc}\left(\frac{2l_7}{\sqrt{3}a_3q}\right); \quad \phi_2 = \mathrm{ArcCsc}\left(\frac{2l_8}{\sqrt{3}a_5r}\right)$$

$$\phi_3 = \mathrm{ArcCsc}\left(\frac{2l_9}{\sqrt{3}a_1p}\right)$$

where 'ArcCsc(·)' implies $\mathrm{Cosec}^{-1}(\cdot)$. Substituting the values of ϕ_1, ϕ_2, and ϕ_3 in Eqs. (A2)–(A4), we get three equations in three variables, a_1p, a_3q and a_5r, which are as follows:

$$\frac{\sqrt{3}}{2}a_1p\,\mathrm{Csc}\left[\frac{\pi}{3} - \mathrm{ArcCsc}\left(\frac{2l_7}{\sqrt{3}a_3q}\right)\right] = l_7 \tag{2}$$

$$\frac{\sqrt{3}}{2}a_3q\,\mathrm{Csc}\left[\frac{\pi}{3} - \mathrm{ArcCsc}\left(\frac{2l_8}{\sqrt{3}a_5r}\right)\right] = l_8 \tag{3}$$

$$\frac{\sqrt{3}}{2}a_5r\,\mathrm{Csc}\left[\frac{\pi}{3} - \mathrm{ArcCsc}\left(\frac{2l_9}{\sqrt{3}a_1p}\right)\right] = l_9 \tag{4}$$

where 'Csc(·)' stands for Cosec(·). Eqs. (2)–(4) can now be solved for a_1p, a_3q and a_5r, which are then substituted in Eq. (A1) to find a, b, and c.

2.2. Step ii

Knowing the positions of the base mobile knots, the coordinates of all the joints on each base mobile knot can be easily determined using the relations provided in Eq. (A5). Since the relative position between the joints on a mobile knot never changes, the coordinate of the joints on plane b can be determined referring to Fig. 4 and using the relations given in Eq. (A6). Similar relations for determining the coordinates of the joints in plane c and d can be obtained depending on the required position of the top mobile knots for gripping an object. For plane c, the coordinates of the joints are given in Eq. (A7).

2.3. Step iii

Knowing the geometry of the base and top platforms, we can solve for the inverse kinematics of the Dodekapod to determine its cylinder lengths for a specific position and orientation of the top platform, and the required positions of the top mobile knots. Initially, the lengths of the base cylinders are either minimum or maximum depending on which one adopts for the initial positions of the base mobile knots. However, during iterations of finding a feasible solution, the positions of the base mobile knots are changed, which can be determined using the following cosine rules (Fig. 3b):

Fig. 4. Projections of a general mobile knot on vertical plane.

$$l_7 = \sqrt{L_a^2 + L_b^2 - 2L_aL_b\cos\left(\frac{2\pi}{3} - \alpha - \beta\right)} \tag{5}$$

$$l_8 = \sqrt{L_b^2 + L_c^2 - 2L_bL_c\cos\left(\frac{2\pi}{3} - \beta - \gamma\right)} \tag{6}$$

$$l_9 = \sqrt{L_a^2 + L_c^2 - 2L_aL_c\cos\left(\frac{2\pi}{3} - \gamma - \alpha\right)} \tag{7}$$

where L_a, L_b, and L_c are defined as

$$L_a \equiv \sqrt{s^2 + a^2}; \quad L_b \equiv \sqrt{s^2 + b^2} \tag{8}$$

$$L_c \equiv \sqrt{s^2 + c^2} \tag{9}$$

and

$$\tan\alpha = \frac{s}{a}; \quad \tan\beta = \frac{s}{b}; \quad \tan\gamma = \frac{s}{c}$$

Similarly, referring to Fig. 3a, the lengths of top cylinders are obtained from:

$$l_{10} = \sqrt{L_{at}^2 + L_{bt}^2 - 2L_{at}L_{bt}\cos\left(\frac{2\pi}{3} - \alpha_t - \beta_t\right)} \tag{10}$$

$$l_{11} = \sqrt{L_{bt}^2 + L_{ct}^2 - 2L_{bt}L_{ct}\cos\left(\frac{2\pi}{3} - \beta_t - \gamma_t\right)} \tag{11}$$

$$l_{12} = \sqrt{L_{at}^2 + L_{ct}^2 - 2L_{at}L_{ct}\cos\left(\frac{2\pi}{3} - \gamma_t - \alpha_t\right)} \tag{12}$$

where L_{at}, L_{bt}, L_{ct}, and $\tan\alpha_t$, $\tan\beta_t$, and $\tan\gamma_t$, are defined similar to Eqs. (8) and (9), respectively, which can be evaluated from the input a_t, b_t, and c_t. We shall now derive the equations to find the lengths of the legs, l_i, for $i = 1, \ldots, 6$. The attachment points between the legs, and the base and top

platforms lie in planes b and c. Their coordinates are already determined with respect to the fixed and movable frame, respectively. Hence, we can solve for the inverse kinematics to determine the leg lengths treating it as a general 6–6 Stewart platform mechanism. Referring to Fig. 5, the base points with respect to frame B, (with the origin at O_b) can be described as

$$\mathbf{b}_i^b \equiv [x_{bi} \quad y_{bi} \quad z_{bi}]^{\mathrm{T}} \tag{13}$$

whereas the top points referring to frame C (with the origin at O_c) are defined as

$$\mathbf{c}_i^c \equiv [x_{\mathbf{c}i} \quad y_{\mathbf{c}i} \quad z_{\mathbf{c}i}]^{\mathrm{T}} \tag{14}$$

for $i = 1, \ldots, 6$. As the points lie in the X–Y plane of their respective frames, for all i's

$$z_{\mathbf{b}i} = z_{\mathbf{c}i} = 0$$

The leg vectors referring to the fixed base frame is given by

$$\boldsymbol{l}_i \equiv [l_{xi} \quad l_{yi} \quad l_{zi}]^{\mathrm{T}} \tag{15}$$

for $i = 1, \ldots, 6$, where the leg lengths are

$$l_i = \|\boldsymbol{l}_i\| = \sqrt{(l_{xi}^2 + l_{yi}^2 + l_{zi}^2)} \tag{16}$$

The position vector representing the origin of frame C, O_c, from the origin of frame B, O_b, as in Fig. 5, is described as

$$\mathbf{t}_c^b = [x \quad y \quad z]^{\mathrm{T}} \tag{17}$$

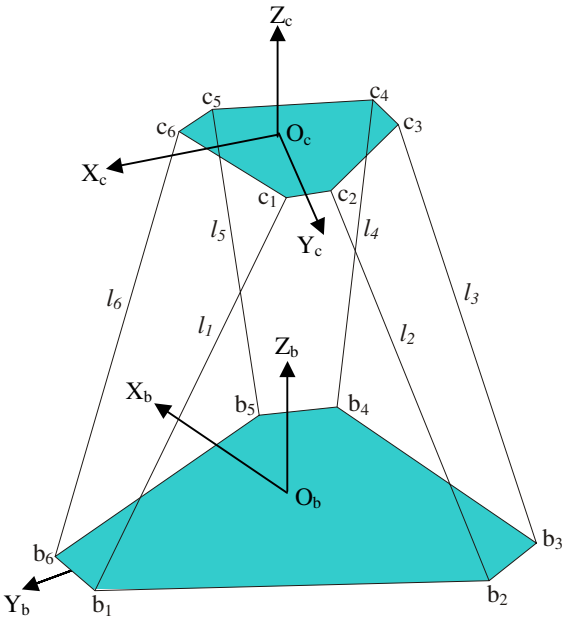

Fig. 5. Dodekapod reduced to a general 6–6 Stewart platform manipulator.

whereas the rotation matrix is

$$R_c^b = \begin{bmatrix} r_{xx} & r_{xy} & r_{xz} \\ r_{yx} & r_{yy} & r_{yz} \\ r_{zx} & r_{zy} & r_{zz} \end{bmatrix} \tag{18}$$

Eqs. (17) and (18), describe the position and orientation of the top platform with respect to the base. We shall now apply transformations to find out the coordinates of the top platform points with respect to the base frame B as

$$\mathbf{c}_i^b = \mathbf{R}_c^b \mathbf{c}_i^c + \mathbf{t}_c^b \tag{19}$$

where $\mathbf{c}_i^b$ is the ith point of the top platform with respect to the base frame. The difference between $\mathbf{c}_i^b$ and $\mathbf{b}_i^b$ gives the leg vector, $\boldsymbol{l}_i$, i.e.,

$$\boldsymbol{l}_i = \mathbf{c}_i^b - \mathbf{b}_i^b$$

or

$$\boldsymbol{l}_i = \mathbf{R}_c^b \mathbf{c}_i^c + \mathbf{t}_c^b - \mathbf{b}_i^b \tag{20}$$

Using Eqs. (16) and (20), we obtain six explicit scalar equations, for $i = 1, \ldots, 6$, as

$$l_i^2 = (r_{xx}x_{\mathbf{c}i} + r_{xy}y_{\mathbf{c}i} + x - x_{\mathbf{b}i})^2 + (r_{yx}x_{\mathbf{c}i} + r_{yy}y_{\mathbf{c}i} + y - y_{\mathbf{b}i})^2 + (r_{zx}x_{\mathbf{c}i} + r_{zy}y_{\mathbf{c}i} + z)^2 \tag{21}$$

which provides the lengths of the six leg cylinders of the Dodekapod under study. Thus, a complete inverse kinematic solution for the Dodekapod is obtained from Eqs. (5)–(7), (10)–(12), and (21).

2.4. Step iv

The feasibility of a solution obtained by solving the inverse kinematics using the method proposed above can be checked by considering the minimum and maximum displacements of each cylinder denoted by $l_{\min}$ and $l_{\max}$, respectively. If the length of at least one of the cylinders exceeds either of the two limits, the solution will not be feasible. Hence, for $i = 1$–12, if, $l_i < l_{\min}$ or $l_i > l_{\max}$ for any one or more values of i, the solution is not feasible. When a solution fails to be feasible then the base mobile knots must be moved to a new position. The following algorithm is used to find the next set of positions of the base mobile knots: Fig. 6 shows possible ranges of positions the base mobile knots can take to give practical solution, i.e.,

- When the base mobile knot is at position u_1, the length of the leg is minimum (Fig. 6a). As the base mobile knot moves outwards from the center of the base platform, the length of the leg increases. Moreover, the length of the leg is maximum at u_2. So, there can be infinite number of solutions between u_1 and u_2. When the leg-length determined from the inverse kinematics calculations with the initial position of the base mobile knots at u_1 is less than the minimum, $l_{\min}$ then the base mobile knots can be displaced outwards from the center of the base platform,

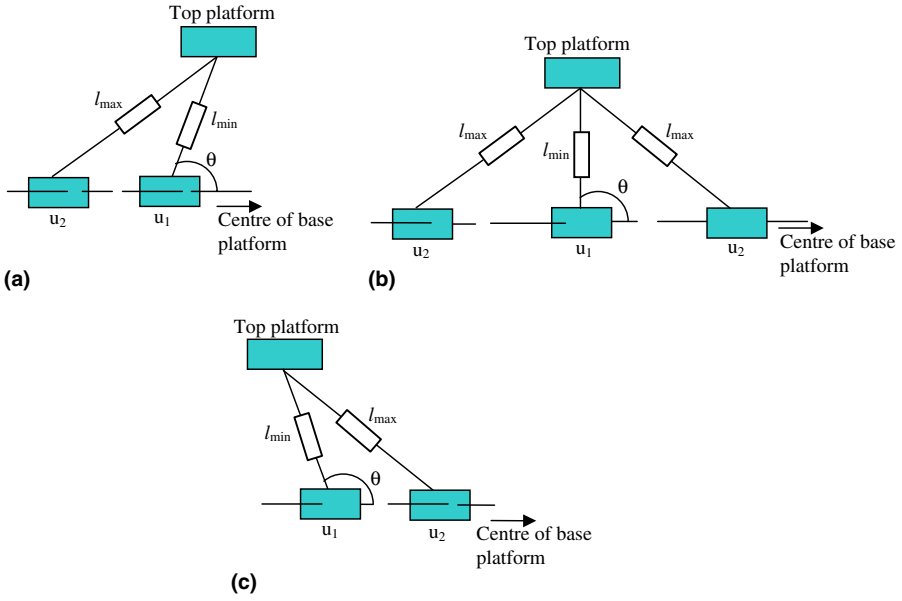

Fig. 6. Range of possible solutions: (a) for $\theta < 90°$, (b) for $\theta = 90°$ and (c) for $\theta > 90°$.

whereas the length of leg is greater than the maximum, l_{max} then the base mobile knots can be moved towards the center of the base.

- There are a few other possible cases too. Firstly, if the leg-length is less than the minimum limit, l_{min} when the axis of the prismatic joint of the leg is perpendicular to the axis of the sliding joint between the base mobile knot and base platform (Fig. 6b), then the leg-length increases in both the directions of movement of the base mobile knots. Secondly, if the maximum leg-length, l_{max} occurs when the axis of the prismatic joint of the leg is perpendicular to the axis of the sliding joint between the base mobile knot and base platform, then there is no other possible solution and the present position of the base mobile knot cannot be changed. If the leg-length is exceeding this maximum limit then the required pose cannot be realized.
- One more possible situation arises if the minimum leg-length, l_{min} is encountered when the angle between the joint axes of the leg and the base mobile knot, i.e., θ is more than 90° (Fig. 6c). In this case the leg-length increases when the joints are moved towards the center of the base platform and decreases when the joints are moved outwards.

From the foregoing discussion the following conclusions regarding the determination of the next position of the base mobile knots can be made as

(i) For angle $\theta < 90°$
  (a) If the leg-length is less than the minimum limit, l_{min} then the base mobile knot connected to that leg must be moved outwards from the center of the base platform.
  (b) If the leg-length is greater than the maximum limit, l_{max}, then the base mobile knot connected to that leg must be moved towards the center of base platform.

(ii) For angle, $\theta = 90°$, if the leg length is less than the minimum limit, then the base mobile knot connected to that leg can be moved either inwards towards the center of the base platform or outwards from it. However, the decision regarding the direction of the knot movement can be taken keeping in view the stability of the system or some other criteria such as the operation that is to be performed on the object gripped while it is held in that pose.

(iii) For angle, $\theta > 90°$
   (a) If the leg-length is less than the minimum limit, $l_{\min}$, then the base mobile knot connected to that leg must be moved towards the center of the base platform.
   (b) If the leg length is greater than the maximum limit, $l_{\max}$, then the required position of the end-effector lies outside the total workspace of the Dodekapod. Hence, the base mobile knot connected to that leg must be moved outwards from the center of the base platform.

For each of the above cases feasible solutions also exist in the regions that are formed by the mirror image of the above described regions about a plane that (i) contains the point b; (ii) is perpendicular to the axis along which the slider moves; and (iii) is parallel to the edge of base platform formed by the joints on the mobile knot. Also, in all the above cases the relationship between the direction of movement of the base mobile knots with the leg-length reverses when the angle θ changes from an acute angle to an obtuse one and vice versa.

3. Forward kinematics

For the purpose of forward kinematics analysis, the Dodekapod can be considered as a special case of Stewart platform with hexagonal top and base platforms having three alternate sides of equal lengths. The forward kinematics problem of the Dodekapod deals with the determination of the position and orientation of the end-effector for a given set of leg-lengths. The total number of variables for which the forward kinematics is required to be solved is nine, three of which are the components of the translation vector and the remaining six are the elements of the rotation matrix. Hence, we need nine equations to solve the forward kinematics problem. Similar to inverse kinematics, the forward kinematics has also been solved using a hierarchical method. First, the positions of the mobile knots which are not affected by the leg-lengths are determined. Then the coordinates of all the attachment points are calculated using the relations developed while solving the inverse kinematics, i.e., Eqs. (A5)–(A7).

3.1. Position of mobile knots

The position of base mobile knots can be determined using Eqs. (2)–(4). Similar equations for the top mobile knots can be derived, which are given as follows: Referring to Fig. 3a, where points $c_1, \ldots, c_6$ coincide with points $d_1, \ldots, d_6$,

$$\frac{\sqrt{3}}{2} c_2 p_t \operatorname{Csc}\left[\frac{\pi}{3} - \operatorname{ArcCsc}\left(\frac{2l_{10}}{\sqrt{3}c_4 q}\right)\right] = l_{10} \tag{22}$$

$$\frac{\sqrt{3}}{2}c_4 q_t \operatorname{Csc}\left[\frac{\pi}{3} - \operatorname{ArcCsc}\left(\frac{2l_{11}}{\sqrt{3}c_6 r}\right)\right] = l_{11} \tag{23}$$

$$\frac{\sqrt{3}}{2}c_6 r_t \operatorname{Csc}\left[\frac{\pi}{3} - \operatorname{ArcCsc}\left(\frac{2l_{12}}{\sqrt{3}c_2 p}\right)\right] = l_{12} \tag{24}$$

Eqs. (22)–(24) can be solved for c_2p_t, c_4q_t, and c_6r_t, and then a_t, b_t and c_t can be calculated similar to a, b, c of Eq. (A1) using Eq. (A8).

3.2. Forward kinematics equations

A rotation matrix is orthogonal, i.e., $(\mathbf{R}_c^b)^{\mathrm{T}}\mathbf{R}_c^b = \mathbf{1}_{3\times3}$–$\mathbf{1}_{3\times3}$ being the 3×3 identity matrix. Equating the (1,1), (1,2) and (2,2) elements of the left and right hand sides of the above orthogonality condition, three constraint equations are obtained. Besides, using these three constraints, the leg-length equation, Eq. (21), can be reduced to the following form:

$$\begin{aligned}&(x^2+y^2+z^2) + 2x_{ci}(r_{xx}x + r_{yx}y + r_{zx}z) + 2y_{ci}(r_{xy}x + r_{yy}y + r_{zy}z)\\ &\quad - 2x_{bi}(x + x_{ci}r_{xx} + y_{ci}r_{xy}) - 2y_{bi}(y + x_{ci}r_{yx} + y_{ci}r_{yy}) + x_{bi}^2 + y_{bi}^2 + x_{ci}^2 + y_{ci}^2 - l_i^2 = 0\end{aligned} \tag{25}$$

for $i = 1,\ldots,6$. Thus, a total of nine equations in nine unknowns, namely, x, y, z, r_{xx}, r_{xy}, r_{yx}, r_{yy}, r_{zx} and r_{zy} are obtained. The last column of the rotation matrix need not be calculated as they are multiplied with vanishing elements of the vectors. These equations are solved numerically using MATHEMATICA. It is, however, noted that the numerical algorithms have the obvious drawback that they cannot be applied to find all the solutions (real and complex) of the problem, and it is impossible to determine the number of solutions for a general case. In this paper, our intention is to find a feasible solution that can be practically implemented in the Dodekapod controller, rather than investigating the all or best solutions. All the nine equations for the forward kinematics are quadratic which have multiple roots. Due to the nonlinearity of these equations, obtaining a closed form solution is very complicated. Hence, a numerical method is used.

4. Numerical example

In this section, a numerical example is taken to demonstrate the inverse and forward kinematics algorithms of the Dodekapod proposed in this paper.

4.1. Inverse kinematics

Here the inverse kinematics of the Dodekapod is solved for a certain position and orientation of the top platform with respect to the base platform. The object gripped is considered to be a cylinder of a diameter such that the top mobile knots are at 300 mm from the center of the platform. The position of the top platform is given as

$$\mathbf{t}_c^b = [\,0 \quad 0 \quad 600\,]^{\mathrm{T}} \tag{26}$$

whereas the Z–Y–Z Euler angles [14] to represent the top platform orientation are 60°, 0° and 0°, respectively. The resulting rotation matrix for this sequence of rotation is then calculated as

$$\mathbf{R}_c^b = \begin{bmatrix} 0.5 & -0.866 & 0 \\ 0.866 & 0.5 & 0 \\ 0 & 0 & 1 \end{bmatrix} \tag{27}$$

We shall now determine the coordinates of all the joints using the equations derived in the preceding sections. All the three base mobile knots are considered to be at 500 mm from the center of the base platform. The value of s = 64 mm. The coordinates of various joints with respect to their local coordinate frames are shown in Table 1. The z-coordinate for all the above is zero as they are expressed in their local coordinate frames.

From Eqs. (5)–(7), we get,

$$l_7 = l_8 = l_9 = 802.025$$

and from Eqs. (10)–(12)

$$l_{10} = l_{11} = l_{12} = 455.615$$

Table 1
Inverse kinematics solutions

Joint	x-coordinate	y-coordinate
a_1	−64	500
a_2	−465.013	−194.574
a_3	−401.013	−305.426
a_4	401.013	−305.426
a_5	465.013	−194.574
a_6	64	500
d_1	64	300
d_2	−64	300
d_3	−291.808	−94.577
d_4	−227.808	−205.426
d_5	227.808	−205.426
d_6	291.808	−94.5744
b_1	−54	554
b_2	−506.778	−230.23
b_3	−452.778	−323.765
b_4	452.778	−323.765
b_5	506.778	−230.23
b_6	54	554
c_1	54	354
c_2	−54	354
c_3	−333.573	−130.23
c_4	−279.573	−223.765
c_5	279.573	−223.765
c_6	333.573	−130.23

Now, using Eq. (21), we determine the lengths of the six leg cylinders as,

$$l_1 = l_2 = l_3 = l_4 = l_5 = l_6 = 621.063$$

It may be observed that when all the cylinders of the Dodekapod are at their minimum positions, the orientation of the top platform is given by the matrix in Eq. (27), and the coordinates along x and y are zero. Hence, in the above example, we get all the leg-lengths equal.

4.2. Forward kinematics

The procedure described in Section 3 is followed to solve the forward kinematics of the Dodekapod. All the equations involved are solved using MATHEMATICA. The lengths of the 12 cylinders are considered as

$$l_1 = l_2 = 700, \quad l_3 = l_4 = 800, \quad l_5 = l_6 = 700$$

$$l_7 = 855, \quad l_8 = 1050, \quad l_9 = 900, \quad l_{10} = 500$$

$$l_{11} = 550, \quad l_{12} = 450$$

Substituting the values of l_7, l_8 and l_9 in Eqs. (2)–(4), and solving the equations, the values of a_1p, a_3q, a_5r are determined as

$$a_1p = 400.136, \quad a_3q = 581.561, \quad a_5r = 630.545$$

Similarly, substituting the values of l_{10}, l_{11} and l_{12} in Eqs. (22)–(24), we get the values of c_2p_t, c_4q_t and c_6r_t as

$$c_2p_t = 228.8, \quad c_4q_t = 344.662, \quad c_6r_t = 289.628$$

Moreover, from Eqs. (A1) and (A8) with $s = s_t = 64$,

$$a = 437.086, \quad b = 618.561, \quad c = 667.495$$

$$a_t = 265.75, \quad b_t = 381.61, \quad c_t = 326.578$$

With these values, the coordinates of the base and top platform attachment points can be computed, which are given in Table 2. Now, all the parameters that are required for solving the basic equations of forward kinematics have been determined. Now these values are substituted in Eq. (25) and then the resulting set of simultaneous non-linear equations are solved numerically with the 'FindRoot' function available in MATHEMATICA, which uses Newton–Raphson method to find the roots of the simultaneous equations.

The solution, thus, obtained is listed below:

$$x = -3.398, \quad y = -139.331, \quad z = 566.153;$$

$$r_{xx} = 0.549, \quad r_{xy} = -0.831;$$

$$r_{yx} = 0.805, \quad r_{yy} = 0.552;$$

$$r_{zx} = -0.223, \quad r_{zy} = -0.057.$$

Table 2
Forward kinematics solutions

Attachment point, b_i	x-coordinate, x_{bi}	y-coordinate, y_{bi}
b_1	−53.999	491.086
b_2	−609.412	−289.488
b_3	−461.881	−329.019
b_4	504.300	−353.515
b_5	651.831	−313.984
b_6	54.000	491.086
On top, c_i	x_{ci}	y_{ci}
c_1	54.000	319.750
c_2	−53.999	319.750
c_3	−404.251	−171.039
c_4	−256.720	−210.570
c_5	209.058	−183.055
c_6	356.589	−143.524

5. Conclusions

In this paper, a hierarchical scheme to solve the inverse and forward kinematics for a new type of parallel manipulator, namely, the 12 degree of freedom Dodekapod, is proposed. The kinematics is solved by separately treating the mechanism to change the position of mobile knots, and a Stewart platform mechanism effecting the required pose of the top platform. The inverse kinematics involves solving for the lengths of the base and top cylinders from the information about the positions of the mobile knots, and then solving for leg-lengths. Similarly, the forward kinematics is solved, first, to find the positions of the mobile knots using the information regarding the base and top cylinder lengths, and then solving for the forward kinematics of a general 6–6 Stewart platform. The algorithms are demonstrated with a numerical example.

Acknowledgments

Authors acknowledge the support provided by the DAAD (German Academic Exchange Program) to the first author during 1999–2000 to carry out the research at the Technical University, Berlin, Germany, under the DAAD-IITs collaboration. Besides the help from Mr. Kiran Kolluru, an M. Tech student at IIT Delhi, to re-draw the figures and re-write the equations during the preparation of the final manuscript is duly acknowledged.

Appendix A

In this appendix, some useful geometric expressions are provided which are essential for the inverse and forward kinematic analyses of the Dodekapod at hand. From Fig. 3b,

$$\left.\begin{aligned} a &= a_1 p + s\tan\left(\tfrac{\pi}{6}\right) \\ b &= a_3 q + s\tan\left(\tfrac{\pi}{6}\right) \\ c &= a_5 r + s\tan\left(\tfrac{\pi}{6}\right) \end{aligned}\right\} \tag{A1}$$

whereas the "sine rules" provides,

$$\frac{l_7}{\sin\left(\frac{2\pi}{3}\right)} = \frac{a_3 q}{\sin\phi_1} = \frac{a_1 p}{\sin\left(\frac{\pi}{3} - \phi_1\right)} \tag{A2}$$

$$\frac{l_8}{\sin\left(\frac{2\pi}{3}\right)} = \frac{a_5 r}{\sin\phi_2} = \frac{a_3 q}{\sin\left(\frac{\pi}{3} - \phi_2\right)} \tag{A3}$$

$$\frac{l_9}{\sin\left(\frac{2\pi}{3}\right)} = \frac{a_1 p}{\sin\phi_3} = \frac{a_5 r}{\sin\left(\frac{\pi}{3} - \phi_3\right)} \tag{A4}$$

Moreover, the coordinates of the six base mobile knots (Fig. 3b) are given as

$$\left.\begin{aligned}
x_{a_1} &= -s \quad y_{a1} = a \\
x_{a_2} &= -\sqrt{s^2 + b^2}\cos\left(\tfrac{\pi}{6} - \beta\right) \\
y_{a_2} &= -\sqrt{s^2 + b^2}\sin\left(\tfrac{\pi}{6} - \beta\right) \\
x_{a_3} &= -\sqrt{s^2 + b^2}\cos\left(\tfrac{\pi}{6} + \beta\right) \\
y_{a_3} &= -\sqrt{s^2 + b^2}\sin\left(\tfrac{\pi}{6} + \beta\right) \\
x_{a_4} &= \sqrt{s^2 + c^2}\cos\left(\tfrac{\pi}{6} + \gamma\right) \\
y_{a_4} &= -\sqrt{s^2 + c^2}\sin\left(\tfrac{\pi}{6} + \gamma\right) \\
x_{a_5} &= \sqrt{s^2 + c^2}\cos\left(\tfrac{\pi}{6} - \gamma\right) \\
y_{a_5} &= -\sqrt{s^2 + c^2}\sin\left(\tfrac{\pi}{6} - \gamma\right) \\
y_{a_6} &= a x_{a_6} = a
\end{aligned}\right\} \tag{A5}$$

Similarly, the coordinates of the base mobile knots in plane b can be expressed from Fig. 4 as

$$\left.\begin{aligned}
x_{b_1} &= x_{a_1} + q \quad y_{b_1} = y_{a_1} + p \\
x_{b_2} &= x_{a_2} - r\cos\left(\tfrac{\pi}{6} + \lambda\right) \\
y_{b_2} &= y_{a_2} - r\sin\left(\tfrac{\pi}{6} + \lambda\right) \\
x_{b_3} &= x_{a_3} - r\cos\left(\tfrac{\pi}{6} - \lambda\right) \\
y_{b_3} &= y_{a_3} - r\sin\left(\tfrac{\pi}{6} - \lambda\right) \\
x_{b_4} &= x_{a_4} + r\cos\left(\tfrac{\pi}{6} - \lambda\right) \\
y_{b_4} &= y_{a_4} - r\sin\left(\tfrac{\pi}{6} - \lambda\right) \\
x_{b_5} &= x_{a_5} + r\cos\left(\tfrac{\pi}{6} + \lambda\right) \\
y_{b_5} &= y_{a_5} - r\sin\left(\tfrac{\pi}{6} + \lambda\right) \\
x_{b_6} &= x_{a_6} - q \quad y_{b_6} = y_{a_6} + p
\end{aligned}\right\} \tag{A6}$$

The coordinates of the top mobile platform in plane c are then given by

$$\left.\begin{aligned}
x_{c_1} &= x_{d_1} + q \quad y_{c_1} = y_{d_1} + p \\
x_{c_2} &= x_{d2} + q \quad y_{c_2} = y_{d_2} + p \\
x_{c_3} &= x_{d_3} - r\cos\left(\tfrac{\pi}{6} + \lambda\right) \\
y_{c_3} &= y_{d_3} - r\sin\left(\tfrac{\pi}{6} + \lambda\right) \\
x_{c_4} &= x_{d_4} - r\cos\left(\tfrac{\pi}{6} - \lambda\right) \\
y_{c_4} &= y_{d_4} - r\sin\left(\tfrac{\pi}{6} - \lambda\right) \\
x_{c_5} &= x_{d_5} + r\cos\left(\tfrac{\pi}{6} - \lambda\right) \\
y_{c_5} &= y_{d_5} - r\sin\left(\tfrac{\pi}{6} - \lambda\right) \\
y_{c_6} &= y_{d_6} - r\sin\left(\tfrac{\pi}{6} + \lambda\right) \\
x_{c_6} &= x_{d_6} + r\cos\left(\tfrac{\pi}{6} + \lambda\right)
\end{aligned}\right\} \tag{A7}$$

where p, q, and r are shown in Fig. 4. Finally, from Fig. 3a the following relations are obtained:

$$\left.\begin{aligned}
a_t &= c_2 p_t + s_t \tan\left(\tfrac{\pi}{6}\right) \\
b_t &= c_4 q_t + s_t \tan\left(\tfrac{\pi}{6}\right) \\
c_t &= c_6 r_t + s_t \tan\left(\tfrac{\pi}{6}\right)
\end{aligned}\right\} \tag{A8}$$

References

[1] G. Spur, E. Uhlmann, M. Seibt, A new type of gripping system with parallel kinematics, Prod. Eng. V/2 (1965) 61–64.

[2] P. Bande, Programming of DODEKAPOD: A Parallel Manipulator, M. Tech Project Report, IIT Delhi, April 2000.

[3] D. Stewart, A platform with 6 degree of freedom, Proc. Inst. Mech. Engrs. 180 (Part 1, No. 15) (1965) 371–386.

[4] V.E. Gough, Contribution to discussion to papers on research in automobile stability and control and in tyre performance, by Cornell Staff, Proc. Auto. Div. Instn. Mech. Engrs (1956–1957) 392–394.

[5] B. Dasgupta, T.S. Mruthyunjaya, A canonical formulation of the direct position kinematics problem for a general 6–6 Stewart platform, Mech. Mach. Theory 29 (6) (1994) 819–827.

[6] M.L. Husty, An algorithm for solving the direct kinematics of the general Stewart–Gough platforms, Mech. Mach. Theory 31 (4) (1996) 365–379.

[7] P. Dietmaier, The Stewart–Gough platform of general geometry can have 40 real postures, in: J. Lenarcic, M.L. Husty (Eds.), Advances in Robot Kinematics: Analysis and Control, Kluwer Publishers, 1998, pp. 7–16, 0-7923-5169.

[8] M. Raghavan, The Stewart platform of general geometry has 40 configurations, J. Mech. Des. 115 (June) (1993) 277–282.

[9] C. Innocenti, Forward kinematics in polynomial form of the general Stewart platform, Proc. of the 1998 DETC ASME Design Eng. Tech. Conf., 25th Biennial Mechanisms Conference, September 13–16, Atlanta, GA, Paper#DETC98/MECH-5894, 1998.

[10] C.M. Gosselin, Kinematische und statische analyse eines ebenen parallelen manipulaters mit dem freiheitsgrad zwei, Mech. Mach. Theory 31 (2) (1996) 149–160.

[11] J. Yang, Z.J. Geng, Closed form forward kinematics solution to a class of Hexapod robot, IEEE Trans. R&A 14 (3) (1998) 503–508.

[12] K. Sugimoto, Computational scheme for dynamic analysis of parallel manipulator, ASME J. Mech. Transmission Automat. Des. 111 (1989) 29–33.
[13] S.K. Saha, W.O. Schiehlen, Recursive kinematics and dynamics for closed loop multibody systems, Int. J. Mech. Struct. Mach. 29 (2) (2001) 143–175.
[14] L. Tsai, Robot Analysis, John Wiley & Sons Inc., New York, 1999.